Chiral Extrapolations of the $\rho(770)$ Meson in $\mathbf{N_f = 2 + 1}$ Lattice QCD Simulations

R. Molina[1], B. Hu[1], M. Doring[1,2], M. Mai[1] and A. Alexandru[1]

(1)   (2)

Contents

Unitarized Chiral Perturbation Theory

- **ChPT expansion of the amplitude for meson-meson scattering**

$$t(s) = t_2(s) + t_4(s) + ..., t_{2k} = \mathcal{O}(p^{2k}) \tag{1}$$

- **Lowest-order Chiral Lagrangian:**

$$\mathcal{L}_2 = \frac{f^2}{4} \langle \partial_\mu U^\dagger \partial^\mu U + M(U + U^\dagger) \rangle \tag{2}$$

- **Next-to-leading order term:**

$$\begin{aligned}
\mathcal{L}_4 &= L_1 \langle \partial_\mu U^\dagger \partial^\mu U \rangle^2 + L_2 \langle \partial_\mu U^\dagger \partial_\nu U \rangle \langle \partial^\mu U^\dagger \partial^\nu U \rangle \\
&+ L_3 \langle \partial_\mu U^\dagger \partial^\mu U \partial_\nu U^\dagger \partial^\nu U \rangle + L_4 \langle \partial U^\dagger \partial^\mu U \rangle \langle U^\dagger M + M^\dagger U \rangle \\
&+ L_5 \langle \partial_\mu U^\dagger \partial^\mu U (U^\dagger M + M^\dagger U) \rangle + L_6 \langle U^\dagger M + M^\dagger U \rangle^2 \\
&+ L_7 \langle U^\dagger M - M^\dagger U \rangle^2 + L_8 \langle M^\dagger U M^\dagger U + U^\dagger M U^\dagger M \rangle
\end{aligned} \tag{3}$$

Unitarized Chiral Perturbation Theory

where $U(\phi) = \exp(i\sqrt{2}\Phi/f)$, and

$$\Phi(x) = \begin{pmatrix} \frac{\pi^0}{\sqrt{2}} + \frac{\eta}{\sqrt{6}} & \pi^+ & K^+ \\ \pi^- & -\frac{\pi^0}{\sqrt{2}} + \frac{\eta}{\sqrt{6}} & K^0 \\ K^- & \bar{K}^0 & -\frac{2}{\sqrt{6}}\eta \end{pmatrix} \tag{4}$$

$$M = \begin{pmatrix} m_\pi^2 & 0 & 0 \\ 0 & m_\pi^2 & 0 \\ 0 & 0 & 2m_K^2 - m_\pi^2 \end{pmatrix} . \tag{5}$$

J. Gasser and H. Leutwyler, Annals Phys. 158, 142 (1984)

J. Gasser and H. Leutwyler, NPB250, 465 (1985)

J. A. Oller, E. Oset and J. R. Pelaez, PRD59, 074001 (1999)

$T(\pi\pi \to \pi\pi)$ **(1 channel) UChPT (NLO) Oller, Oset, Pelaez (1999)**

V_{IAM} is the kernel of the scattering equation:

$$T = T + VGT \longrightarrow T = [I - V_{\mathrm{IAM}}G]^{-1}V_{\mathrm{IAM}}, \text{ with}$$

$$V_{\mathrm{IAM}} = [1 - V_4(V_2)^{-1}]^{-1}V_2$$

$$V_2 = \frac{m_\pi^2 - s}{f_\pi^2}$$

$$V_4 = -\frac{4}{f^4}((2L_1 + L_3)(s - 2m_\pi^2)^2$$
$$+ L_2((t - 2m_\pi^2)^2 + (u - 2m_\pi^2)^2)$$
$$+ 2(2L_4 + L_5)m_\pi^2(s - 2m_\pi^2) +$$
$$4(2L_6 + L_8)m_\pi^4)$$

- $I = 1, L = 1$:

$$\longrightarrow \boxed{V(\pi\pi) = -2p^2/(3(f_\pi^2 - 8\hat{l}_1 m_\pi^2 + 4\hat{l}_2 E^2))} \qquad (6)$$

and, $\qquad \hat{l}_1 = 2L_4 + L_5 \qquad \hat{l}_2 = 2L_1 - L_2 + L_3.$

Unitarized Chiral Perturbation Theory (Two channels: $\pi\pi$, $K\bar{K}$)

- **Potential** (p-wave, $I = 1$, $\pi\pi$, $K\bar{K}$):

$$V_2(W) = - \begin{pmatrix} \frac{2p_\pi^2}{3f_\pi^2} & \frac{\sqrt{2}p_K p_\pi}{3f_K f_\pi} \\ \frac{\sqrt{2}p_K p_\pi}{3f_K f_\pi} & \frac{p_K^2}{3f_K^2} \end{pmatrix} , \qquad (7)$$

$$V_4(W) = - \begin{pmatrix} \frac{8p_\pi^2(2\hat{l}_1 m_\pi^2 - \hat{l}_2 W^2)}{3f_\pi^4} & \frac{8p_\pi p_K(L_5(m_K^2 + m_\pi^2) - L_3 W^2)}{3\sqrt{2}f_\pi^2 f_K^2} \\ \frac{8p_\pi p_K(L_5(m_K^2 + m_\pi^2) - L_3 W^2)}{3\sqrt{2}f_\pi^2 f_K^2} & \frac{4p_K^2(10\hat{l}_1 m_K^2 + 3(L_3 - 2\hat{l}_2)W^2)}{9f_K^4} \end{pmatrix} .$$

- **Scattering equation**: $\boxed{T = V_2[V_2 - V_4 - V_2 G V_2]^{-1} V_2}$

$$S = \begin{pmatrix} \eta e^{2i\delta_1} & i(1-\eta^2)^{1/2}e^{i(\delta_1+\delta_2)} \\ i(1-\eta^2)^{1/2}e^{i(\delta_1+\delta_2)} & \eta e^{2i\delta_2} \end{pmatrix} \qquad T_{ij} = -\frac{8\pi W}{2i\sqrt{p_i p_j}}(S_{ij} - \delta_{ij})$$

Pion mass dependence of the meson decay constants

One loop SU(3) UChPT,

$$f_\pi = f_0 \left[1 - 2\mu_\pi - \mu_K + \frac{4M_{0\pi}^2}{f_0^2} \left(L_4^r + L_5^r \right) + \frac{8M_{0K}^2}{f_0^2} L_4^r \right]$$

$$f_K = f_0 \left[1 - \frac{3\mu_\pi}{4} - \frac{3\mu_K}{2} - \frac{3\mu_\eta}{4} + \frac{4M_{0\pi}^2}{f_0^2} L_4^r + \frac{4M_{0K}^2}{f_0^2} \left(2L_4^r + L_5^r \right) \right]$$

$$f_\eta = f_0 \left[1 - 3\mu_K + \frac{4L_4^r}{f_0^2} \left(M_{0\pi}^2 + 2M_{0K}^2 \right) + \frac{4M_{0\eta}^2}{f_0^2} L_5^r \right]$$
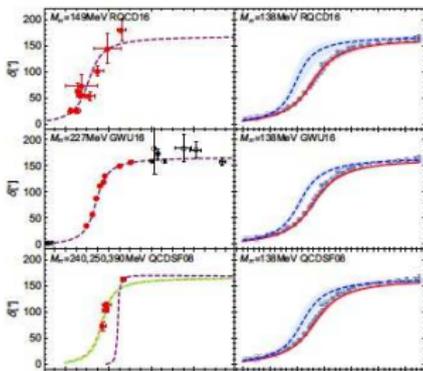
J. Nebreda and J. R. Pelaez., Phys. Rev. D **81**, 054035 (2010)

Correlations in the energy levels:

$$\boxed{\chi^2 = (\vec{W}_1 - \vec{W}_0)^T C^{-1} (\vec{W}_1 - \vec{W}_0)}$$

$$W_{1i} = \frac{g(W_{0i}) - f(W_{0i})}{f'(W_{0i}) - g'(W_{0i})} + W_{0i} \; .$$

Analysis of $N_f = 2$ lattice data: RQCD, GWU, QCDSF, Lang, ETMC and CP-PACS
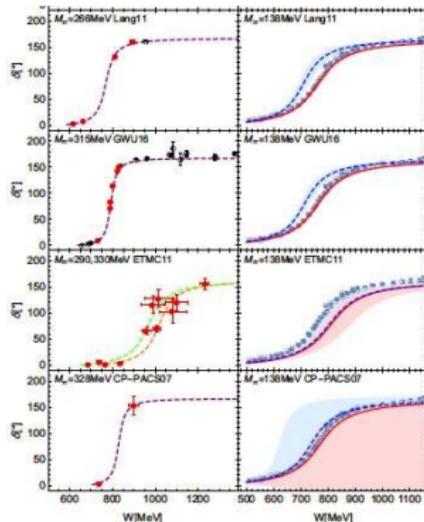
$K\bar{K}$ channel included a posteriori (red)

B. Hu, R. Molina, M. Döring and A. Alexandru, PRL**117** (2016)

G. S. Bali et al. [RQCD Collaboration], PRD93, 054509 (2016)
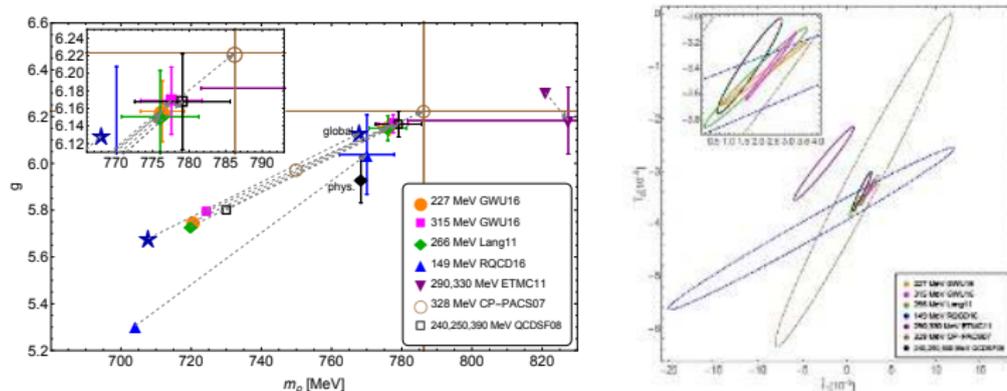D. Guo, A. Alexandru, R. Molina and M. Doring, PRD94, 034501 (2016)
M. Göckeler et al. [QCDSF Collaboration], PoS LATTICE 2008, 136 (2008)
C. B. Lang, D. Mohler, S. Prelovsek and M. Vidmar, PRD84, 054503 (2011)
X. Feng, K. Jansen and D. B. Renner [ETMC Collaboration], PRD83, 094505 (2011)
S. Aoki et al. [CP-PACS Collaboration], PRD76, 094506 (2007)

Analysis of $N_f = 2$ lattice data: RQCD, GWU, QCDSF, Lang, ETMC and CP-PACS

Figure: Left: Effect of the $K\bar{K}$ channel in the (m_ρ, g) plane indicated with arrows, after chiral extrapolation to the physical pion mass. Right: error ellipses in the $(\hat{l}_1, \hat{l}_2)$ plane.

Most ellipses in the $(\hat{l}_1, \hat{l}_2)$ plane from the $N_f = 2$ lattice data analysis have a common overlap area.

$K\bar{K}$ **loops in** $\pi\pi \to \pi\pi$
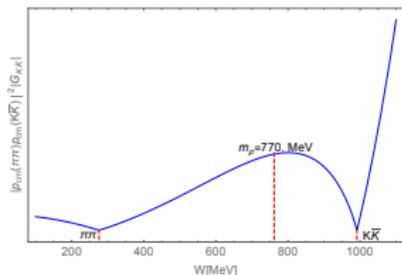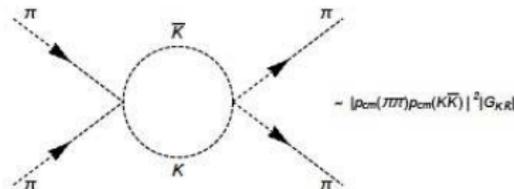
Ratio of the couplings of the ρ meson to $\pi\pi$ and $K\bar{K}$

	Oller/Pelaez1999	Guo/Oller2012
$\left| g_{K\bar{K}}/g_{\pi\pi} \right|$	0.54	0.64

NL0 UChPT (PRD59) vs. One-loop UChPT (PRD84)

Not that small!

$N_f = 2 + 1$ **lattice data analysis (UChPT)**

[1.] D. J. Wilson, R. A. Briceño, J. J. Dudek, R. G. Edwards and C. E. Thomas, Phys. Rev. D **92**, 094502 (2015). [Wilson15] [Str1-4]

[2.] J. J. Dudek *et al.* [Hadron Spectrum Collaboration], Phys. Rev. D **87**, no. 3, 034505 (2013). [Dudek13] [Str1,3,4]

[3.] J. Bulava, B. Fahy, B. Hörz, K. J. Juge, C. Morningstar and C. H. Wong, Nucl. Phys. B **910**, 842 (2016). [Bulava16] [Str1-3]

[4.] J. Bulava, B. Hörz, B. Fahy, K. J. Juge, C. Morningstar and C. H. Wong, PoS LATTICE **2015**, 069 (2016). [Bulava15] [Str1-3]

[5.] S. Aoki *et al.* [CS Collaboration], Phys. Rev. D **84**, 094505 (2011). [Aoki11] [Str1-3]

[6.] C. Alexandrou *et al.*, arXiv:1704.05439 [hep-lat] (2017). [Alexandrou17] [Str3]

[7.] Z. Fu and L. Wang, Phys. Rev. D **94**, no. 3, 034505 (2016). [Fu16] [Str3]

[8.] T. Metivet [Budapest-Marseille-Wuppertal Collaboration], PoS LATTICE **2014**, 079 (2015). [BMW] (large errors-not analyzed)

Minimization Strategies

- **[Str1]** Four parameters are left free: $\hat{l}_1$, $\hat{l}_2$, L_3 and L_5; Individual fits.
- **[Str2]** L_5 is fixed. Combined fit of all data for $m_\pi \leq 300$ MeV.
- **[Str3]** L_3 and L_5 are fixed. Individual fits.
- **[Str4]** L_3 and L_5 are fixed.[1] Combined fit of the Hadron Spectrum Collaboration data for $m_\pi = 235$ and 390 MeV.

---

[1] Values from a fit to experimental phase shift data from $\pi\pi$, πK, $K\bar{K}$..., M. Döring, U.-G. Meißner and W. Wang, JHEP **1310**, 011 (2013). "Experimental fit"

Minimization strategy 1 (four free parameters)

Strong non trivial correlations, many χ^2 minima, best extrapolation to the physical point is selected.

	M_π(MeV)	$\hat{l}_1$	$\hat{l}_2$	L_3	L_5	$\chi^2_{\text{d.o.f.}}$
				[Str1]		
[Wilson15]	236	$4.7^{+1.2}_{-0.8}$	$-3.0^{+0.2}_{-0.9}$	$-3.4^{+1.7}_{-0.2}$	$-0.4^{+0.6}_{-1.0}$	1.0
[Dudek13]	391	$5.4^{+0.9}_{-0.1}$	$-7.4^{+0.6}_{-0.1}$	$+4.3^{+0.3}_{-0.04}$	$-3.8^{+0.7}_{-0.1}$	1.3
[Bulava16]	230	$6.3^{+1.1}_{-1.0}$	$-3.0^{+0.3}_{-0.4}$	$-3.5^{+0.4}_{-0.3}$	$-1.5^{+0.8}_{-1.0}$	1.3
[Bulava15]	280	$6.3^{+1.8}_{-0.2}$	$-3.0^{+0.5}_{-1.4}$	$-3.0^{+3.3}_{-0.2}$	$-0.4^{+1.0}_{-0.6}$	1.4
[Aoki11]	300 & 400	$2.1^{+3.8}_{-1.2}$	$-3.0^{+0.5}_{-1.9}$	$-3.2^{+1.2}_{-0.6}$	$0.7^{+0.7}_{-6.3}$	1.4
[Alexandrou17]	317	$13.3^{+0.8}_{-0.4}$	$-12.9^{+0.5}_{-0.3}$	$15.0^{+0.3}_{-0.1}$	$-11.7^{+0.7}_{-0.4}$	0.7
[Str2]	≤ 300	$4.7^{+0.9}_{-0.5}$	$-2.9^{+0.2}_{-0.1}$	$-3.26^{+0.13}_{-0.06}$	$0.64^{(f)}$	2.2
Experimental	138	0.26 ± 0.05	-3.96 ± 0.04	-3.01 ± 0.02	0.64 ± 0.03	-

Table: Low-energy constants and $\chi^2_{\text{d.o.f.}}$ obtained in minimization strategy 1 and 2 for the $N_f = 2 + 1$ lattice data analyzed.

A very good exptrapolation in the UChPT model is possible, HOWEVER, some of the lattice data sets have VERY DIFFERENT values of the LECs. More constraints in the LECs needed.
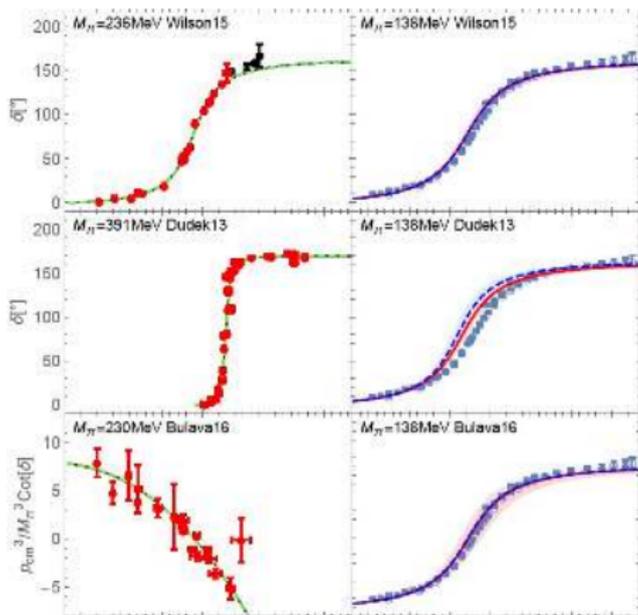
Minimization strategy 2 (L_5 fixed)
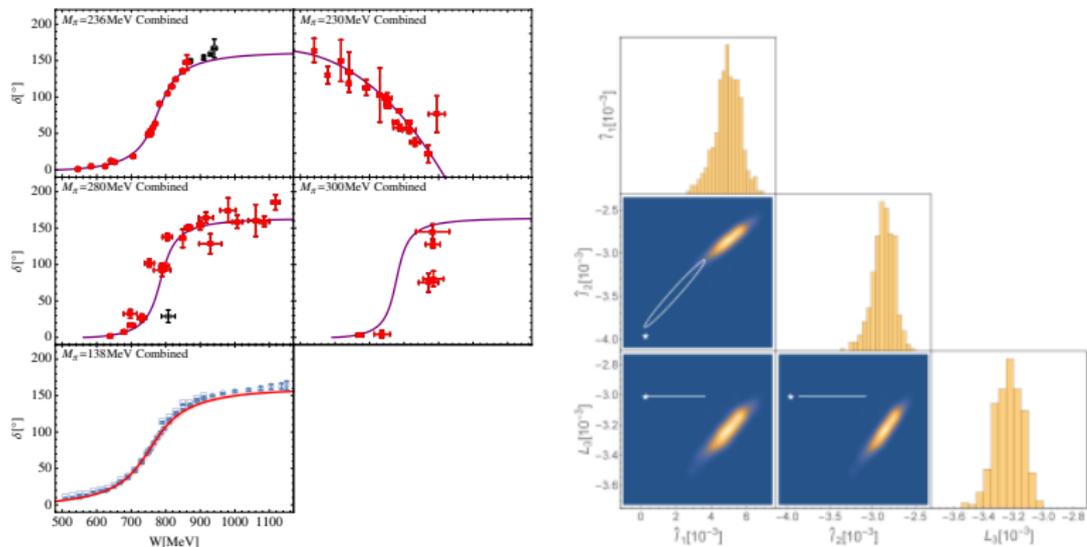
Figure: Left: Phase shifts obtained for the minimization strategy 2. Lattice data included in the fit are [Wilson15], [Bulava16], [Bulava15], [Aoki11]. Right: Density histogram from resampling obtained in minimization 2. Ellipses in white show the result obtained in the fit of the $N_f = 2$ data, [Lang11], with the SU(2) UChPT model. The star indicates the experimental fit.
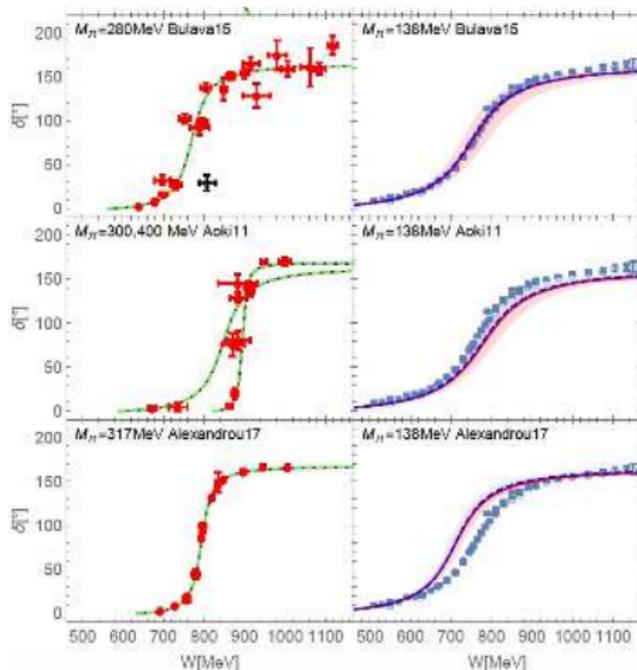
Minimization strategy 2 (L_5 fixed)

- Strong correlations between $\hat{l}_1$, $\hat{l}_2$ and L_3 are detected.
- In the common fit for $m_\pi \leq 300$ MeV, [Aoki11] data are not well described.
- $\chi^2/\mathrm{d.o.f} = 2.2$: there are tensions between [Wilson15], [Bulava15/16] and [Aoki11].
- Differences with the values of the LECs from a fit to experimental phase shift data from $\pi\pi$, $K\bar{K}$, πK,... ($N_f = 2$ lattice data closer to the experimental point). Could be solved: 1) Fitting simultaneously lattice data from other reactions where these LECs are also involved. 2) Lattice determinations of f_π, f_K for the lattice data analyzed. (New constraints)

Minimization strategy 3 (L_3 and L_5 fixed)

Figure: Left: Lattice data included in the fit are marked in red [Wilson15], [Dudek13], [Bulava16]. Right: Extrapolation to the physical point in comparison to the experimental data.

# Minimization strategy 3 (L_3 and L_5 fixed)

Figure: Left: Lattice data included in the fit are marked in red [Bulava15], [Aoki11] and [Alexandrou17]. Right: Extrapolation to the physical point in comparison to the experimental data (red).

Minimization strategy 3 (L_3 and L_5 fixed)

|	M_π (MeV)	[Str3] $(L_3 = -3.01^{(f)}, L_5 = 0.64^{(f)})$		
		$\hat{l}_1$	$\hat{l}_2$	$\chi^2_{\mathrm{d.o.f.}}$
[Wilson15]	236	3.7 ± 1.2	-3.2 ± 0.3	0.9
[Dudek13]	391	1.8 ± 0.5	-3.7 ± 0.3	1.2
[Bulava16]	230	5 ± 2	-3.1 ± 0.4	1.1
[Bulava15]	280	5.7 ± 1.3	-2.9 ± 0.4	1.2
[Aoki11]	300 & 400	2.5 ± 0.7	-2.8 ± 0.3	1.1
[Alexandrou17]	317	2.8 ± 0.8	-3.8 ± 0.3	0.6
[Str4]	236 & 391	2.0 ± 0.2	-3.6 ± 0.1	1.1
[Guo16] ($N_f = 2$)	226 & 315	2.26 ± 0.14	-3.44 ± 0.03	1.3

Table: Low-energy constants and $\chi^2_{\mathrm{d.o.f.}}$ obtained in minimization strategies 3 and 4 for the $N_f = 2 + 1$ lattice data. The superscript (f) indicates parameters held fixed at their experimental values. In the last row, the results from the analysis of the GWU $N_f = 2$ lattice data are shown for comparison.

Minimization strategy 3 (L_3 and L_5 fixed)
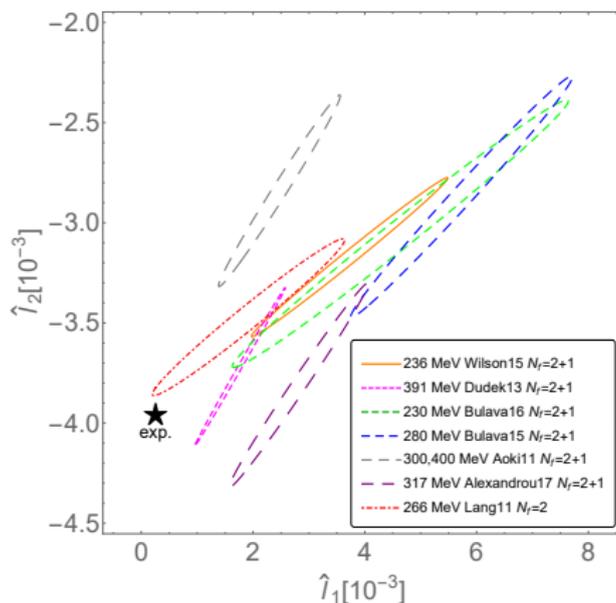
Figure: Error ellipses (68% confidence) in the minimization 3 for the SU(3) analyses of the $N_f = 2 + 1$ lattice data sets. The red dash-dotted ellipse (Lang11) represents the uncertainties from the analysis of the $N_f = 2$ data using a one-channel SU(2) UChPT model.

Minimization strategy 3
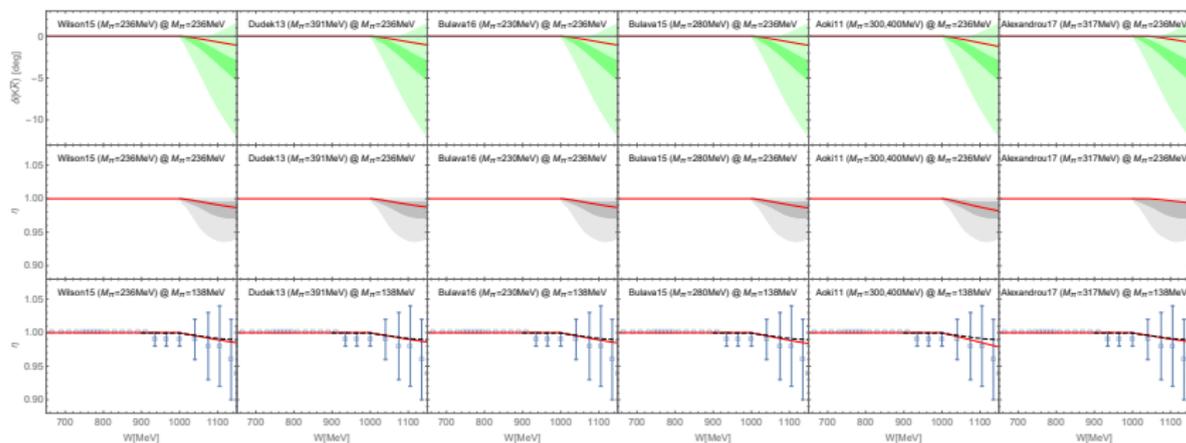
Figure: $K\bar{K}$-phase shifts (first row) and inelasticities (second row) obtained in the minimization strategy 3 for the different lattice data sets extrapolated at $M_\pi = 236$ MeV, in comparison with the result from [Wilson15] (bands). In the bottom row, the extrapolated inelasticity to the physical point, in comparison with the experimental data (squares), and with the Roy-Steiner solution (black-dashed lines) is shown.

Minimization strategy 3 (L_3 and L_5 fixed)

- The minimization is stable compared to strategy 1.
- The values of the LECs are similar for the several $N_f = 2 + 1$ data sets and similar to the ones found in $N_f = 2$ analysis:
- $\hat{l}_2$ has a value of $[-4 - (-3)] \times 10^{-3}$
- $\hat{l}_1$ is $[2 - 4] \times 10^{-3}$ (except [Bulava15/16] $[5 - 6] \times 10^{-3}$)
- SU(2) and SU(3) analysis show similar results, indicating that the $K\bar{K}$ dynamics can be absorved in the SU(2) LECs for $V(\pi\pi)$.
- The extrapolaed ρ mass of the [Dudek13] data is 25 MeV lighter (~ 745 MeV) than the experimental.
- The extrapolaed ρ mass of the [Alexandrou17] data is 50 MeV lighter (~ 720 MeV).

Minimization strategy 4 (L_3 and L_5 fixed)

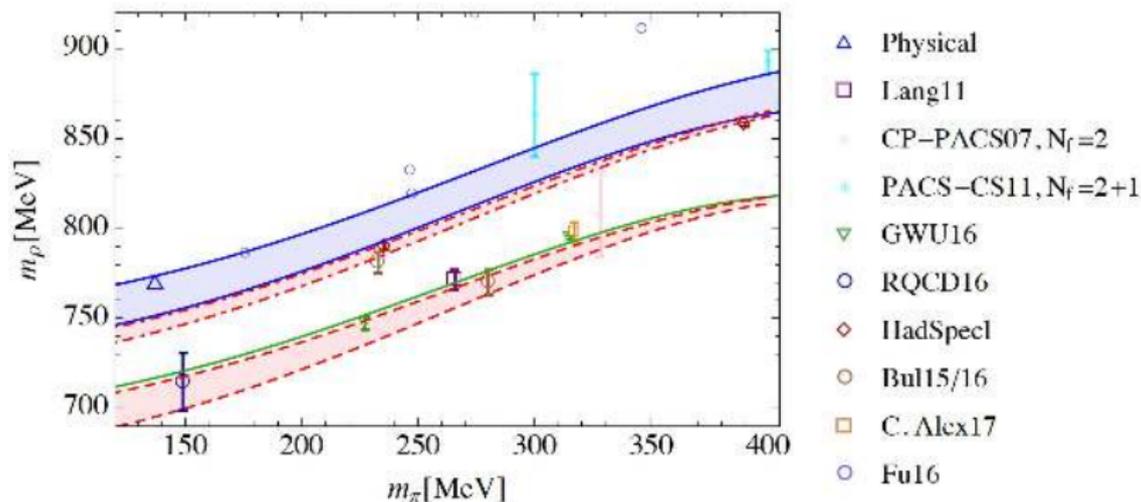Combined fit of the Hadron Spectrum Col. data $m_\pi = 236, 391$ MeV
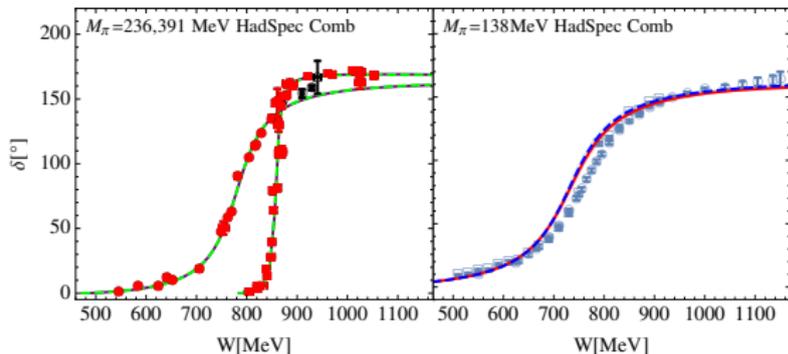
Figure: Left: Lattice data included in the fit are marked in red [Wilson15] and [Dudek13]. Right: Extrapolation to the physical point in comparison to the experimental data.

$$\chi^2/\mathrm{d.o.f} = 1.1$$

The extrapolated ρ mass is ~ 20 MeV lighter (~ 750 MeV) than the experiment.

Pion mass dependence of the ρ meson mass

Figure: Pion mass dependence of the ρ meson mass as prediction of the combined fit of the data of [Wilson15] and [Dudek13] (red dotdashed upper band), in comparison with the result from the $N_f = 2$ analysis of the GWU (blue continues band and green curve, PRD94,034501), and with lattice data. The lower red band is the prediction in strategy (d) when the $K\bar{K}$ channel is removed.

Minimization strategy 4 (L_3 and L_5 fixed)

- The pion mass dependence of the ρ mass obtained from a combined fit of the [Wilson15], [Dudek13] data is COMPATIBLE with most of the $N_f = 2$ lattice data when the $K\bar{K}$ channel is removed

- The analysis reveals tensions with [Bulava15/16] in the sense that these data do not predict a growing ρ mass with pion mass, as observed also in $N_f = 2$ data

- From all the $N_f = 2 + 1$ data, [Bulava15] ($m_\pi = 280$ MeV) and [Alexandrou17] ($m_\pi = 317$ MeV) are closer to the $N_f = 2$ curve of $m_\rho(m_\pi)$.

Coupling, g, versus ρ mass
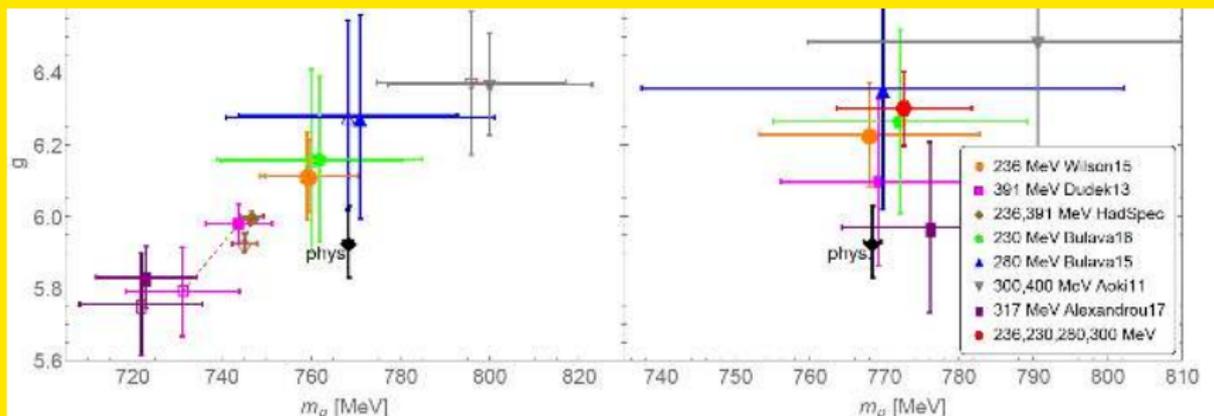
Left: minimization strategies 3 and 4; Right: 1 and 2. In the left figure, empty and filled symbols represent SU(2) and SU(3) analyses respectively. The experimental point is indicated as "phys.". In the right figure, the red hexagon shows the result from minimization 2.

$N_f = 2$ **vs.** $N_f = 2+1$ **lattice data in the UChPT model**

$N_f = 2$ lattice data

- Have a common overlap area in the $(\hat{l}_1, \hat{l}_2)$ plane

- The ρ mass clearly grows with the m_π

- Most data fall in the same $m_\rho(m_\pi)$ curve

- The coupling g is close to the experimental point

- The ρ mass is lighter than the experimental point ($m_\rho \simeq 710$ MeV) for simulations close to the physical point [Bali] ($m_\pi = 149$ MeV)
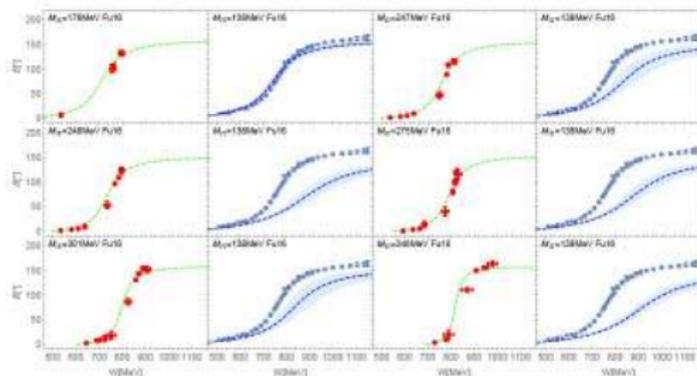
$N_f = 2+1$ lattice data

- Do not have a common overlap area in the $(\hat{l}_1, \hat{l}_2)$ plane

- The ρ mass do NOT GROW with m_π for [Bulava15/16], [Alexandrou17]. But It GROWS for [Wilson15][Dudek13]

- Some of the $N_f = 2+1$ data are closer to the $N_f = 2$ $m_\rho(m_\pi)$ curve ([Bulava15], [Alexandrou17])

- UChPT predics a $m_\rho \simeq 750$ MeV at the physical point from [Wilson15]/[Dudek13]

Conclusions

* ⋆ We find tensions between most of the $N_f = 2 + 1$ lattice data analyzed with the UChPT model, but NOT between $N_f = 2$ data
* ⋆ However, there is mutual agreement between [Wilson15]/[Dudek13] data and $N_f = 2$ lattice data when the $K\bar{K}$ channel is removed/included, with $\Delta m_\rho \simeq 40 - 50$ MeV, and close values of the LECs

Fu16 data

Figure: First and third columns: phase shifts obtained in the SU(2) UChPT fits of the lattice data [Fu16]. The respective pion masses are indicated. Second and fourth columns: Respective chiral extrapolations to the physical point in comparison with the experimental data.

These data show discrepancies with other lattice data sets. In addition, they produce large values of the LECs in comparison with other data sets, and the UChPT extrapolation is far from the experiment.